CREATIVE SCIENCE

Journal home page: csj.snru.ac.th

The interacted characteristically study of alpha, proton, neutron, and gamma radiation against Gd_2O_3-Na_2O-Al_2O_3-P_2O_5 glass system doped with Dy^{3+}: Theoretical investigation

Wuttichai Chaiphaksa[1, 2], Wasu Cheewasukhanont[1, 2], Supakit Yonphan[1, 2], Keerati Kirdsiri[1, 2], Jakrapong Kaewkhao[1, 2], Natthakridta Chanthima[1, 2, *]

[1]Physics Program, Faculty of Science and Technology, Nakhon Pathom Rajabhat University, Nakhon Pathom, 73000 Thailand
[2]Center of Excellence in Glass Technology and Materials Science (CEGM), Nakhon Pathom Rajabhat University, Nakhon Pathom, 73000 Thailand
[*]**Corresponding Author**: natthakridta@webmail.npru.ac.th
DOI: 10.55674/cs.v15i3.251507

Received: 29 January 2023; **Revised:** 11 May 2023; **Accepted:** 5 June 2023; **Available online:** 1 September 2023

Abstract

The radiation shielding properties and fast neutron removal cross-sections of Na_2O-Gd_2O_3-Al_2O_3-P_2O_5 glass system doped with Dy^{3+} were calculated by theoretical approach using the Phy-X program. However, charged particles were simulated via SRIM coding. The result found that density and molar volume of the samples increase with increasing of Dy_2O_3 concentrations. For radiation shielding properties, increasing Dy_2O_3 concentrations impact with the mass attenuation coefficient (MAC), effective atomic number (Z_{eff}), and effective electron density (N_{eff}) and also corresponds to the gamma energy ranges. In other hands, increasing density and the MAC are not result directly with neutron cross-sections. For charged particles, the total mass stopping power (TMSP) of both particle as proton and alpha particles depend on the medium that charged particles traversed and also rely on number of ions.

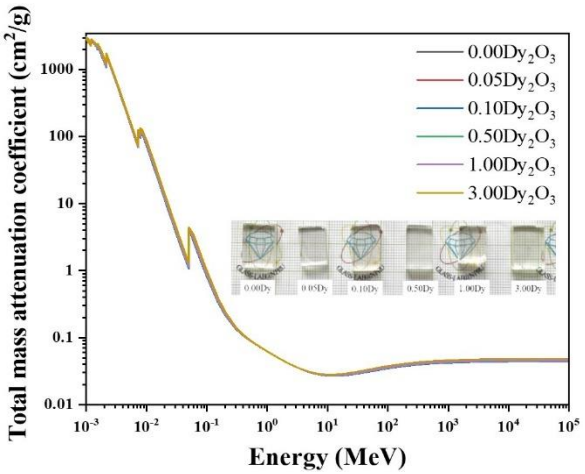

Keywords: Radiation shielding glass; Fast neutron removal cross-sections; Charged particles; Phy-X; SRIM simulation

1. Introduction

For decades, various fields such as nuclear science, nuclear medicine technology, and diagnostic imaging medical applications have availed of radiation [1, 2]. The high-photon energy protections are fundamental to primary respect for the radiological worker, which is one of the most considerable securements [3]. Generally, lead (Pb) and concretes used to be standard materials for the radiation protections owing to its advantages demonstrated as the high-density material, which become the main property improved to attenuate the high-photon energy [4, 5]. Unfortunately, both lead (Pb) and concrete are opaque materials, and toxicity to the creature's DNA is stored in the nucleus of a cell [1, 4, 6]. However, glass is one of the

materials that showed the high-transparent property and improved density by varying chemical composition, which K. Singh, M.I. Sayyed, and several researchers also developed glass formula being glass radiation shielding materials [1, 2, 7]. Typically, the transformation of glass found silica (SiO_2) occurs upon glass structures. Glass components consisting of SiO_2 are in the system, affecting the high melting temperature. For phosphate glasses (P_2O_5), they have especially characterized optical properties as high luminescence, gain density, good chemical durability, and good transparency to visible light regions [7]. In addition, when added Al_2O_3 in P_2O_5 glass structures, it improves to reduce thermal expansion coefficient and results in rising cross-links to PO_4 tetrahedral. Moreover, adding Na_2O which behaved to be network modifier into glass structures can reduce the melting temperature and reducing defects and bubbles [7, 8]. To study the radiation and neutron shielding properties including the interaction of charged particles (proton and alpha particles). The glass specimens that concise of heavy elements are essential requirements for radiation's attenuation [2, 9, 10]. For lanthanide ion (Ln^{3+}), Dy_2O_3 (Dy^{3+}) and Gd_2O_3 (Gd^{3+}) that varied in the glass specimens are important compounds for neutron and radiation shielding [11]. The NIST Center for Neutron Research represented the scattering lengths and cross sections of Gd and Dy, which illustrate the higher thermal neutron cross-sections than other elements [12]. In the light this situation, the glass specimen compositions as $x Dy_2O_3 : 10Gd_2O_3 : 20Na_2O : 10Al_2O_3 : (60–x)P_2O_5$ (DGNAP) were investigated the radiation and neutron shielding properties by theoretical computation from Phy-X software. For charged particles calculations, they were simulated using the SRIM coding for the mass stopping power (TMSP).

2. Materials and Methods

The MQT used for melting the DGNAP glass specimens as composition $xDy_2O_3 : 10Gd_2O_3 : 20Na_2O : 10Al_2O_3 : (60–x)P_2O_5$ by varying Dy_2O_3 concentration at 0.00, 0.05, 0.10, 0.50, 1.00, and 3 mol%. The chemical composition ratios were weighted at 20 gram and put the chemical into the porcelain crucibles. The temperature for melting the DGNAP specimens was utilized at 1,200 °C for 4 h. Then, take the crucible out to pour glass liquid into the stainless-steel mould that was preheated at room temperature, and bring the specimens annealed at 300 °C for 3 h (see in Fig 1). Afterward, take the specimens to cut and polish on the size 1 × 1.5 × 0.3 cm^3 (see in Fig 2).

Finally for experiments, the density measurement used the Archimedes' principle via the equation (1).

$$\rho = \frac{w_a}{w_a - w_b} \times \rho_{liquid} \qquad (1)$$

where w_a, w_b and ρ_{liquid} identify the glass sample's weight in air and liquid, correspond to density of liquid, respectively. In addition, the molar volume used to relate between molecular weight (M_T) of each sample by each sample's density which follows the equation (2).

$$M_{volume} = \frac{M_T}{\rho} \qquad (2)$$

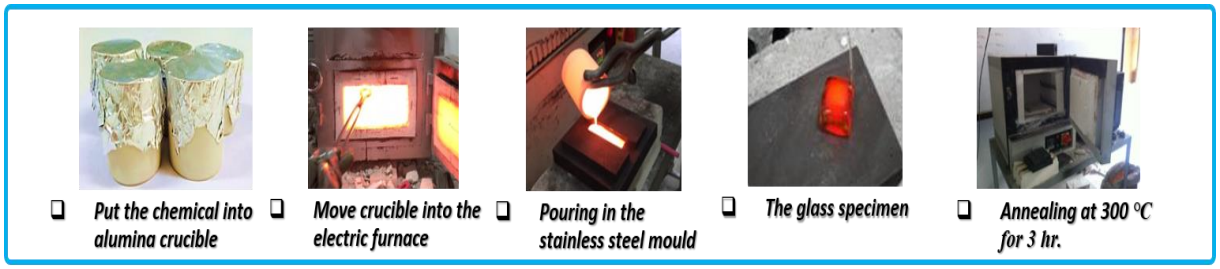

Fig. 1 The melt quenching technique (MQT) processes.

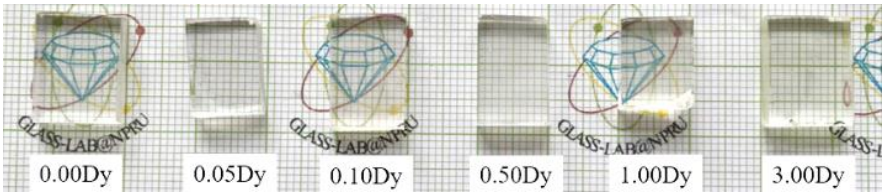

Fig. 2 The DGNAP glass specimens as different concentrations of Dy_2O_3.

The radiation shielding properties computations of the DGNAP glasses used the theoretical calculation by Phy-X program, which developed for calculation of all parameters relevant to shielding and dosimetry [13]. The program bases equation on the mixture rule as the total mass attenuation coefficient (MAC) calculation on equation (3).

$$MAC = (\mu / \rho) = \sum_i w_i (\mu / \rho)_i \qquad (3)$$

The program also generated the effective atomic number (Z_{eff}) and effective electron density (N_{eff}) values by corresponding to the equation (4) and (5), respectively.

$$Z_{eff} = \frac{\sigma_{t,a}}{\sigma_{t,el}} \qquad (4)$$

$$N_{eff} = \frac{MAC}{\sigma_{t,el}} \qquad (5)$$

where $\sigma_{t,a}$ and $\sigma_{t,el}$ referred to the total atomic cross-section (barn/atom) and the total electronic cross-section (barn/electron), respective [14]. Moreover, the program can represent the fast neutron removal cross section (FNRC) [3], which based on the equation (6).

$$\sum_R = \sum_i \rho_i \left(\sum_R / \rho\right)_i \qquad (6)$$

where ρ_i and $\left(\sum_R / \rho\right)_i$ are the partial density and mass removal cross section of the i^{th} constituent, respectively. However, the SRIM program simulation used to simulate the charged particle's interaction also conclude the total mass stopping power (TMSP) and projected ranges of H^+ ions and He^{2+} ions, which the program based the equation (7) on the TMSP simulation [3, 15].

$$\frac{dE}{dx}(MeV / m) = 4\pi r_0^2 z^2 \frac{mc^2}{\beta^2} NZ \left[\ln\left(\frac{2mc^2}{I}\beta^2\gamma^2\right) - \beta^2\right] \qquad (7)$$

3. Results and Discussion

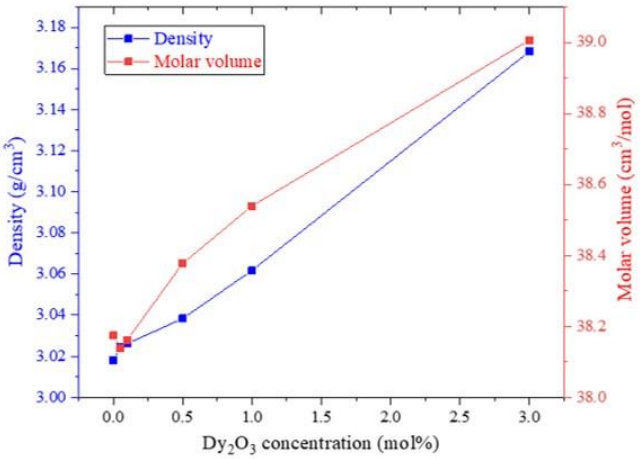

Fig. 3 Density & molar volume plotted with different of Dy_2O_3 concentrations.

From the glass formula as $xDy_2O_3 : 10Gd_2O_3 : 20Na_2O : 10Al_2O_3 : (60–x)P_2O_5$, when P_2O_5 is replaced by Dy_2O_3 concentrations. it affected to all components in glass ratios decrease (see in Table 1). However, density of each glass sample increase with increasing Dy_2O_3 concentrations owing to higher molecular weight of Dy_2O_3 atom than P_2O_5 that is replaced [16]. Likewise, the sample's molar volumes also rise when Dy_2O_3 concentrations and density increase. Due to Dy_2O_3 atoms that rise in glass structure destroy the bonding oxygen. Therefore, bridge of oxygen in glass networks are lost compactness and called non-bridging oxygen (NBO) (see in Fig. 3) [17].

Table 1 The chemical composition of the DGNAP glass specimens.

Mol%	The chemical composition (weight%) of the DGNAP glass					Density (g cm^{-3})	Molar volume (cm^3 mol^{-1})
	Dy_2O_3	Gd_2O_3	Na_2O	Al_2O_3	P_2O_5		
0.00	0.0000	0.2517	0.0861	0.0708	0.5914	3.0180	38.1741
0.05	0.0013	0.2515	0.0860	0.0707	0.5905	3.0245	38.1381
0.10	0.0025	0.2513	0.0859	0.0707	0.5895	3.0262	38.1624
0.50	0.0125	0.2498	0.0854	0.0703	0.5820	3.0383	38.3777
1.00	0.0248	0.2479	0.0848	0.0697	0.5728	3.0618	38.5389
3.00	0.0722	0.2407	0.0823	0.0677	0.5372	3.1682	39.0061

The radiation shielding properties

Table 2 The DGNAP glasses absorption edges of the energies in keV.

Elements	Z	M5	M4	M3	M2	M1	L3	L2	L1	K
Na	**11**	-	-	-	-	-	-	-	-	1.0721
Al	**13**	-	-	-	-	-	-	-	-	1.5596
P	**15**	-	-	-	-	-	-	-	-	2.1455
Gd	**64**	1.1852	1.2172	1.5440	1.6883	1.8808	7.2428	7.9303	8.3756	50.2391
Dy	**66**	1.2949	1.3325	1.6756	1.8418	2.0468	7.7901	8.5806	9.0458	53.7885

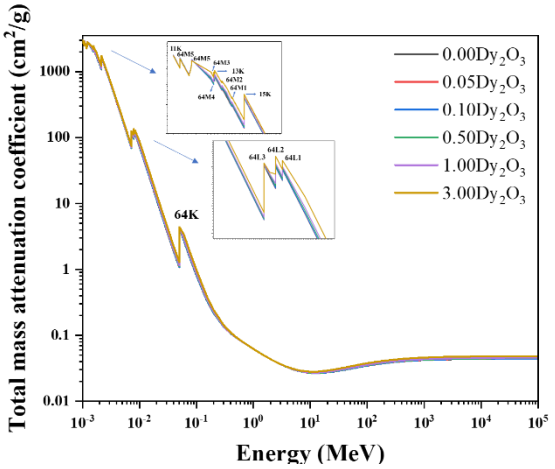

Fig. 4 The mass attenuation coefficient (MAC) plotted with energy and different concentrations of Dy_2O_3.

The MAC that calculated from the Phy-X program is an important parameter which shows the material's radiation shielding ability. Fig. 4 showed the MAC result found that the values a little bit increase when Dy_2O_3 concentrations increase. For gamma radiation shielding, the slightly increased density affected the shielding properties as higher Zeff and Neff. These parameters when they increased affect directly the probability of attenuating gamma radiation. Anyway, adding more Dy_2O_3 in the glass host should be considered for glass forming. However, those value trends decrease to discontinue at low energy ranges, which appeared the characteristic absorption edges of elements in the glass structure as M5 to L1 shells (1.1852 keV, 1.2172 keV, 1.5440 keV, 1.6883 keV, 1.8808 keV, 7.2428 keV, 7.9303 keV, 8.3756 keV, 8.3756 keV, and K shell at 50.2391 keV) of gadolinium (Gd), and 1.2949 keV, 1.3325 keV, 1.6756 keV, 1.8418 keV, 2.0468 keV, 7.7901 keV, 8.5806 keV, 9.0458 keV, and K shell at 53.7885 keV of dysprosium (Dy), respectively. For sodium (Na), aluminium (Al), and phosphate (P) occurred the absorption edges at the K shell as 1.0721 keV, 1.5596 keV, 2.1455 keV (see in Table 2). The occurred absorption edge corresponds to the unique of atom. In addition, it relied on the atomic number of the elements and the energy of the photon and revealed the electron density and electron binding energy in the material.

The Z_{eff} values that calculated from the Phy-X program referred to the number of the electron per atom that interacts with matters in the glass material. Moreover, the radiation shielding properties of materials required the high MAC and Z_{eff} values. In this case, when

Dy_2O_3 concentrations increase, the Z_{eff} improve at all energy ranges (see in Fig. 5). As a result, adding Dy_2O_3 atom in these glasses will create electron surrounding in glass structure for raising interaction probability.

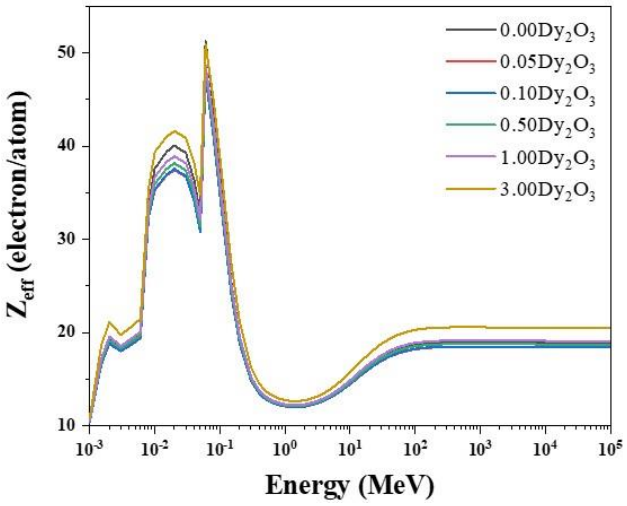

Fig. 5 The effective atomic number (Z_{eff}) plotted with energy and different concentrations of Dy_2O_3.

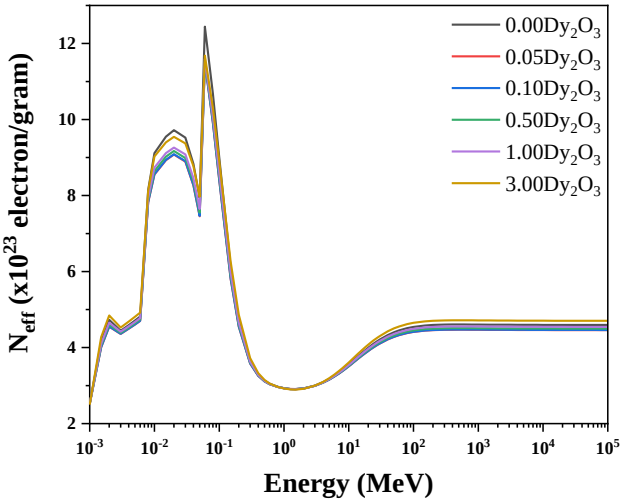

Fig. 6 The effective electron density (N_{eff}) plotted with energy and different concentrations of Dy_2O_3.

The N_{eff} result from the Phy-X program represented the number of electrons per unit mass that interacts between photon energy with matters in the shielding materials. The result found that the characteristics of N_{eff} are the same trends as Z_{eff} values. The discovery of this study indicates that Neff is dependent on the energy range of gamma rays. At low energy range, the photoelectric absorption is predominant and the photon energy is transferred completely with electron bounding. However, the Compton scattering is major on the middle energy range. The photon energy decreases via the collisions and scattering, which Dy_2O_3 atoms result to decrease scattering energy in middle energy ranges (see in Fig. 6). Generally, collisions for decreasing energy scattering disappear on the high energy ranges (> 1.022 MeV), pair production will appear in this energy range [18]. As a result, increasing Dy_2O_3 concentrations is gained in the interaction probability in these energy ranges.

Fast neutron removal cross-section (FNRC)

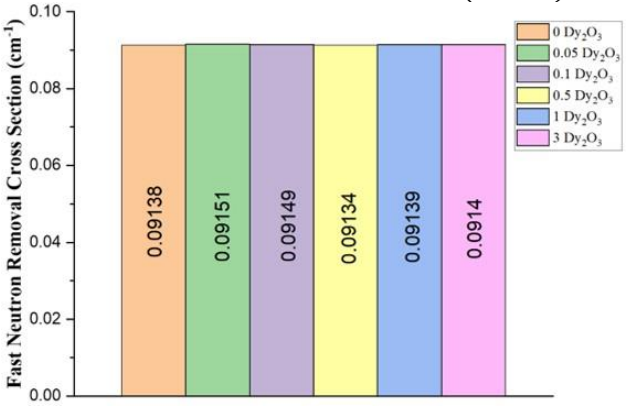

Fig. 7 Fast neutron removal cross-section (FNRCS) of the DGNAP glass specimens.

Fig. 7 showed the FNRCS values plotted with difference of Dy_2O_3 concentrations. The result found that the Phy-X program represented the FNRCS values of each the DGNAP glasses at 0.09138 cm^{-1} (0.00Dy), 0.09151 cm^{-1} (0.05Dy), 0.09149 cm^{-1} (0.10Dy), 0.09134 cm^{-1} (0.50Dy), 0.09139 cm^{-1} (1.00Dy), and 0.09140 cm^{-1} (3.00Dy). Also in this case, with increasing density, and the MAC value by the increased Dy_2O_3 concentrations are not affect directly with the fast neutron cross-section values.

The total mass stopping power (TMSP)

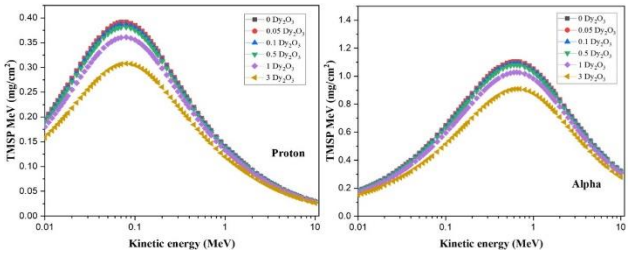

Fig. 8 The total mass stopping power (TMSP) of proton ($^{1}_{1}\mathrm{H}$) and alpha ($^{4}_{2}\mathrm{He}$) via Dy_2O_3 concentration difference of the DGNAP glass specimens.

The results from the SRIM simulations found that the TMSP values of both $^{1}_{1}\mathrm{H}$ ion and $^{4}_{2}\mathrm{He}$ ions decrease with increasing Dy_2O_3 concentrations. Fig. 8 when Dy_2O_3 concentrations increase, it results to density increase but the TMSP of both $^{1}_{1}\mathrm{H}$ ion and $^{4}_{2}\mathrm{He}$ ions decrease. It indicates that it expresses the rate of energy loss of the charged particle per density of the medium traversed [3, 15]. However, alpha particle showed the higher TMSP values than proton due to the TMSP value corresponds to the number of ions which alpha charged particle ($^{4}_{2}\mathrm{He}$) are higher than proton particle $^{1}_{1}\mathrm{H}$.

4. Conclusion

The density and molar volume results of the DGNAP glasses increase with increasing Dy_2O_3 concentrations. The result from the Phy-X program can calculate the radiation shielding parameters as the MAC, Z_{eff}, N_{eff}, and neutron cross-sections values of the DGNAP glass specimens by varying Dy_2O_3 concentrations in the glass structure. It concluded that the MAC, Z_{eff}, and N_{eff} were affected by increasing Dy_2O_3 concentrations and depended on the gamma-ray energy ranges. Increasing density and the MAC value are not involved directly with the fast neutron cross-section. The result from SRIM coding can simulate the TMSP of charged particles of proton and alpha particles. It concluded that both particles express the rate of energy loss of the charged particle per density of the medium traversed and corresponded to the number of ions.

5. Acknowledgement

Authors would like to thanks Thailand Science Research and Innovation (TSRI), Nakhon Pathom Rajabhat University and National Research Council of Thailand for supporting this research (project number TSRI_66_1.2).

6. References

[1] M.I. Sayyed, H.O. Tekin, M.M. Taki, M.H.A. Mhareb, O. Agar, E. Şakar, K.M. Kaky, Bi_2O_3-B_2O_3-ZnO-BaO-Li_2O glass system for gamma ray shielding applications, Optik (Stuttg). 201 (2020) 163525.

[2] A. Khanna, S.S. Bhatti, K.J. Singh, K.S. Thind, Gamma-ray attenuation coefficients in some heavy metal oxide borate glasses at 662 keV, Nucl. Instruments Methods Phys. Res. Sect. B Beam Interact. with Mater. Atoms. 114 (1996) 217 – 220.

[3] W. Cheewasukhanont, K. Siengsanoh, P. Limkitjaroenporn, W. Chaiphaksa, The properties of silicate glass specimens for photon, neutron, and charged particles shielding : The roles of Bi_2O_3, Radiat. Phys. Chem. 201 (2022) 110385.

[4] K.J. Singh, N. Singh, R.S. Kaundal, K. Singh, Gamma-ray shielding and structural properties of PbO-SiO_2 glasses, Nucl. Instruments Methods Phys. Res. Sect. B Beam Interact. with Mater. Atoms. 266 (2008) 944 – 948.

[5] U. Kaur, J.K. Sharma, P.S. Singh, T. Singh, Comparative studies of different concretes on the basis of some photon interaction parameters, Appl. Radiat. Isot. 70 (2012) 233 – 240.

[6] O. Agar, M.I. Sayyed, F. Akman, H.O. Tekin, M.R. Kaçal, An extensive investigation on gamma ray shielding features of Pd/Ag-based alloys, Nucl. Eng. Technol. 51 (2019) 853 – 859.

[7] K. Kaur, K.J. Singh, V. Anand, Correlation of gamma ray shielding and structural properties of PbO-BaO-P_2O_5 glass system, Nucl. Eng. Des. 285 (2015) 31 – 38.

[8] I.El. Mesady, S. Alawsh, Optical and luminescence properties of silicon doped

alumino-phosphate-sodium glass system, J. Non. Cryst. Solids. 482 (2018) 236 – 242.
[9] P. Kaur, D. Singh, T. Singh, Heavy metal oxide glasses as gamma rays shielding material, Nucl. Eng. Des. 307 (2016) 364 – 376.
[10] P. Kaur, K.J. Singh, S. Thakur, P. Singh, B.S. Bajwa, Investigation of bismuth borate glass system modified with barium for structural and gamma-ray shielding properties, Spectrochim. Acta - Part A Mol. Biomol. Spectrosc. 206 (2019) 367 – 377.
[11] S. Kaewjang, U. Maghanemi, S. Kothan, H.J. Kim, P. Limkitjaroenporn, J. Kaewkhao, New gadolinium based glasses for gamma-rays shielding materials, Nucl. Eng. Des. 280 (2015) 21 – 26.
[12] Neutron scattering lengths and cross sections, https://www.ncnr.nist.gov/ resources/n-lengths, 13 October 2021.
[13] E. Şakar, Ö.F. Özpolat, B. Alım, M.I. Sayyed, M. Kurudirek, Phy-X / PSD: Development of a user friendly online software for calculation of parameters relevant to radiation shielding and dosimetry, Radiat. Phys. Chem. 166 (2020) 108496.
[14] W. Cheewasukhanont, P. Limkitjaroenporn, M.I. Sayyed, S. Kothan, H.J. Kim, J. Kaewkhao, High density of tungsten gadolinium borate glasses for radiation shielding material: Effect of WO_3 concentration, Radiat. Phys. Chem. 192 (2022) 109926.
[15] F. Ziegler, P. Biersack, D. Ziegler, SRIM the Stopping and Range of Ion in Matter, SRIM Co., Chester, Maryland 2008.
[16] M. Shoaib, R. Rajaramakrishna, G. Rooh, N. Chanthima, H.J. Kim, C. Saiyasombat, R. Botta, N. Nuntawong, S. Kothan, J. Kaewkhao, Structural and luminescence study of Dy^{3+} doped phosphate glasses for solid state lighting applications, Opt. Mater. (Amst). 109 (2020) 110322.
[17] N. Chanthima, Y. Tariwong, J. Kaewkhao, N. Sangwaranatee, White light emission of Bi_2O_3-B_2O_3-P_2O_5 glasses doped with Dy^{3+}Ion, Mater. Today Proc. 43 (2018) 2498 – 2507.
[18] N. Chanthima, J. Kaewkhao, Investigation on radiation shielding parameters of bismuth borosilicate glass from 1 keV to 100 GeV, Ann. Nucl. Energy. 55 (2013) 23 – 28.